Pis'ma v ZhETF, vol. 93, iss. 1, pp. 13 – 17 © 2011 January 10

Low-temperature conductance of the weak junction in InAs nanowire in the field of AFM scanning gate

A. A. Zhukov[+], *Ch. Volk*[+*], *A. Winden*[+*], *H. Hardtdegen*[+*], *Th. Schäpers*[+*]

[+] *Institute of Solid State Physics RAS, 142432 Chernogolovka, Russia*

[+] *Institute of Bio- and Nanosystems (IBN-1): Forschungszentrum Jüelich, 52425 Jülich, Germany*

[*] *JARA-Fundamentals of Future Information Technology, Forschungszentrum Jülich, 52425 Jülich, Germany*

Submitted 1 November 2010
Resubmitted 19 November 2010

We investigate the conductance of InAs nanowire in the presence of electrical potential created by AFM scanning gate at helium temperature. An influence of local electrical field direction on the tunneling rate through the weak junction in InAs wire is observed clearly. To explain this behavior the redistribution of the electrons among conductive channels in the wire must be taken into account. We confirmed that Coulomb blockade diamonds pattern gives the same result for quantum dot sizes ratio as reveals scanning gate imaging as well.

In the past decade an increasing number of publications were dedicated to investigations of electronic transport in semiconductor nanowires. Due to their small size these one-dimensional objects are very promising for future nanoelectronic and nanophotonic applications. InAs wires [1, 2], in particular, are in the focus of interest not only because these wires have surface charges accumulation layer similar to InN wires [3] but also because of the possibility to alter electronic density and conductivity by a voltage applied to a gate. This feature allows to construct field-effect transistors based on InAs wires. Recently, detailed investigations of the dependence of electronic conductance of InAs wire on their diameter have been performed [1, 4]. In Ref. [2] single electron tunneling and Coulomb blockade in a quantum dot made of InAs wire between the InP is reported. No charging of the single-electron transistor-like effect is observed in homogeneous InAs [2] showing absence of Schottky barrier in between InAs wire and metallic contacts [5]. Conductive scanning probe microscopy has been used to investigate distance-dependent electron transport behavior in InAs nanowires at room temperature [6]. Two regimes of transport behavior were observed. For distances less than 200 nm, the resistance was independent of the distance, thus ballistic electron transport was observed. For greater distances, the resistance was observed to increase linearly with distance, as expected for conventional drift transport.

Scanning probe techniques proved themselves as effective methods to study conductivity properties of low-dimensional structures such as 2D quantum dots (QD) [7 – 9], quantum point contacts [10, 11], QD made of carbon nanotubes [12, 13] and praphene [14]. However, so far there is only one work dedicated dedicated to the investigation of the influence of a charged scanning probe tip on conductivity of an InAs wire at cryogenic temperatures [15].

In this paper we study two field-effect transistors based on InAs wires. According to our experimental data both devices contain one weak junction (presumably a growth defect) dividing each InAs wire into two serial QD. Measurements of the conductance map of devices as function of source to drain voltage (V_{SD}) and back-gate voltage (V_{BG}) allow to estimate sizes of QD. These results will be compared to scanning gate imaging (SGI) which allow to reveal the exact positions of QD under investigation. We investigate the influence of local Coulomb potential altered with charged tip of the scanning probe microscope on tunneling rate through the weak junction as well.

The InAs undoped nanowires were fabricated using metal-organic vapor-phase epitaxy [16]. The diameter of the wires is 100 nm for device A and 120 nm for device B. The wires are placed on a Si n^+ (100) wafer capped with a 100 nm thick SiO_2 insulating layer. The doped silicon substrate serves as the back gate to change the electronic density in the wire with applying a back gate voltage V_{BG}. The evaporated Ti/Au contacts to the wires and the markers of the search pattern are defined by electron-beam lithography. The distances in between contacts are 2 μm and 1.5 μm for devices A and B, respectively. A scanning electron microscopy image of device A is presented in Fig.1a.

All measurements are performed at 4.2 K. Scanning gate imaging measurements are made with home-built scanning probe microscope [17]. All SGI measurements

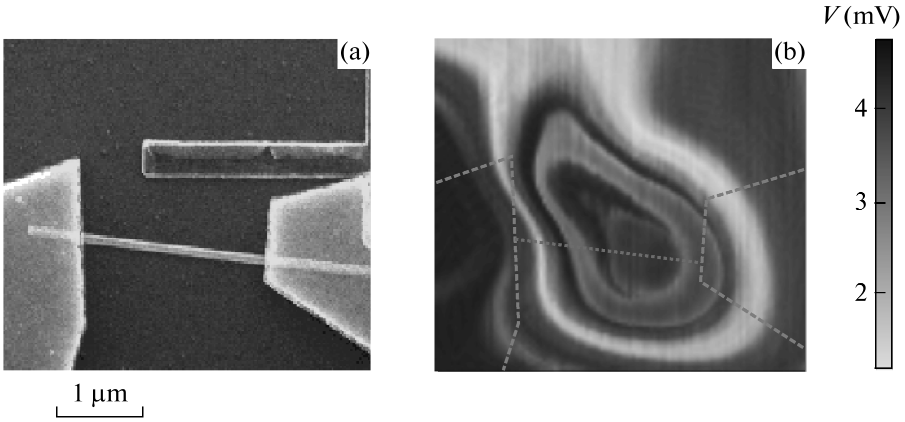

Fig.1. (a) Scanning electron microscope image of device A. The metallic stripe above InAs wire is a part of the search pattern marker. (b) SGI of devices A made at 4.2 K. Driving voltage of 10 mV is applied through 10 MΩ resistor, source to drain voltage V_{SD} is measured during the charged tip scanning. A tip voltage of $V_t = 1$ V and back gate voltage of $V_{BG} = 0$ V is maintained. For both images the scale bar corresponds to 1 μm. Dotted line denotes the wire position and dashed lines denote outline of metallic contacts

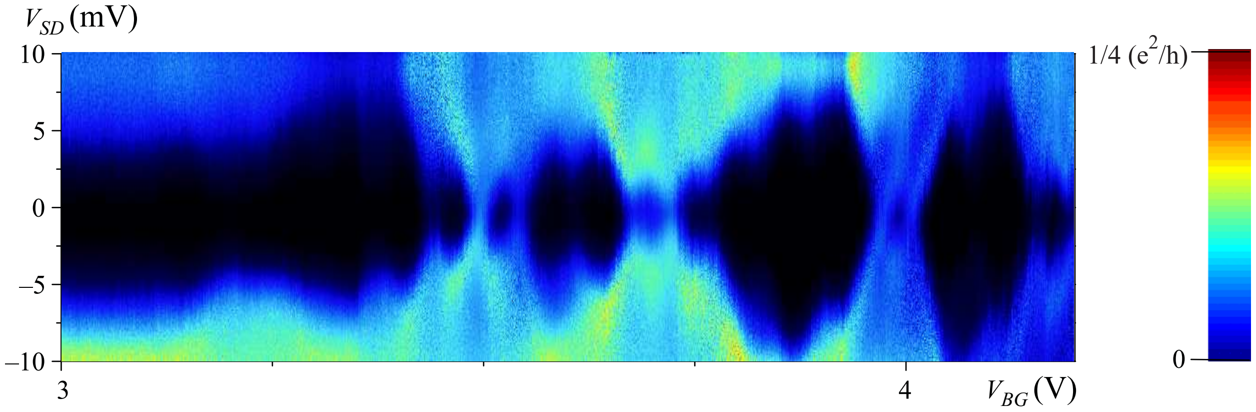

Fig.2. Conductance map of device A measured at 4.2 K as function of source to drain voltage and back gate voltage. Double Coulomb blockade pattern revealing two serial quantum dots in device A is presented at $V_{BG} > 3.3$ V

are performed by keeping the potential of the scanning probe microscope tip (V_t) and V_{BG} constant. The electrical scheme of the SGI experiment is explained in detail in Ref. [13]. Scanning for SGI is performed by keeping the tip 200 nm above SiO_2 surface to eliminate any mechanical or electrical contact of the tip to the wire under investigation.

The conductance of the wire during the scanning is measured using two probe scheme with standard lock-in technique. In case of current-driven SGI measurement (device A) we measure V_{SD} while scanning by applying a current through 10 MΩ resistor. The bias voltage is $V_{AC} = 10$ mV. In case of voltage-driven SGI measurement (device B) we measure the current while scanning applying voltage $V_{AC} = 0.1$ mV.

In addition to the SGI measurements the differential conductance of the nanowires was measured as a function of V_{SD} and V_{BG}. Here, a driving voltage of $V_{AC} = 0.1$ mV is used while the current is measured with the current amplifier.

In Fig.2 the conduction map as the function of V_{SD} and V_{BG} of the device A is presented. The larger diamonds of the Coulomb blockade present at all values of back gate voltages come from the smaller dot in the wire. A closer look on Fig.2 reveals that at $V_{BG} > 3.3$ V an additional Coulomb blockade pattern with smaller period arises. We attribute this additional pattern to the presence of the larger dot in the wire.

Device A revealed a conduction map as function of V_{SD} and V_{BG} which is typical for two quantum dots with negligible mutual capacitance [18, 19]; a similar behavior was observed in InAs wires by Bleszynski *et al.* [15]. This behavior is the result of the small thickness ($d = 100$ nm) of the silicon oxide insulating layer ($d \ll l_L, l_S$), compared to the lengths l_L and l_S of the larger and smaller dots, respectively. From the ratio of

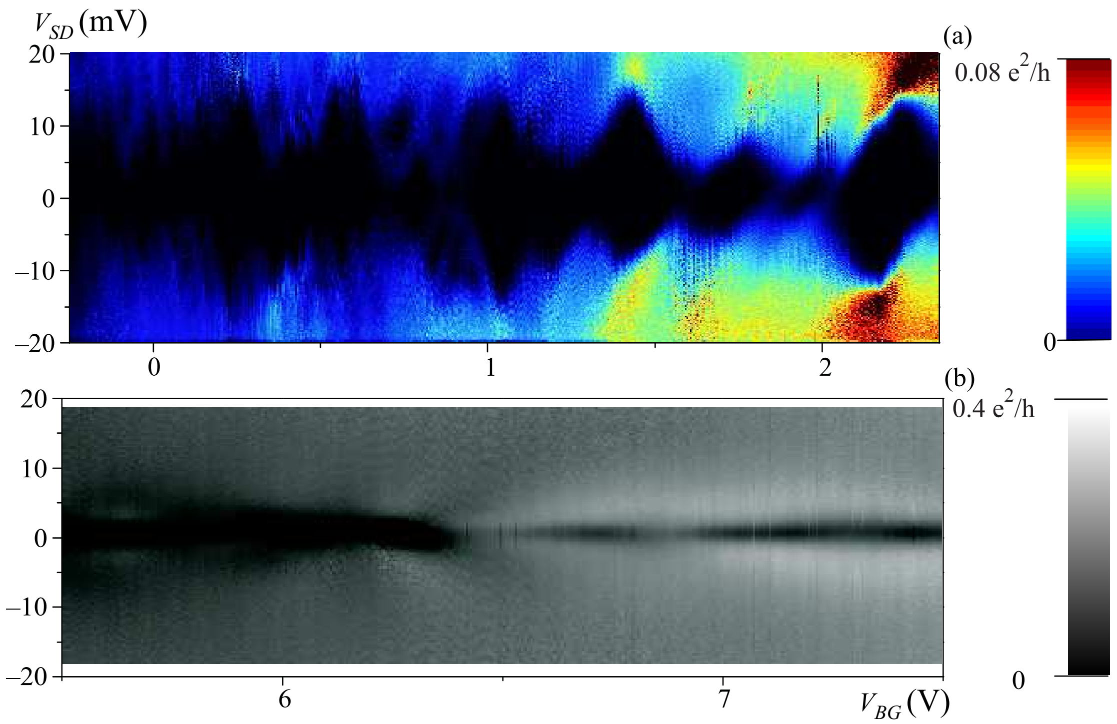

Fig.3. (a) Conductance map of device B as function of source to drain voltage and back gate voltage at low back gate voltages. At $V_{BG} < 1.1$ V double Coulomb blockade pattern indicates two serial quantum dots formed in device B. (b) Conductance map of device B as function of V_{SD} and V_{BG}, both dots are completely open

Coulomb blockade ($\Delta V_S/\Delta V_L = c_{W-BG,L}/c_{W-BG,S}$) we can estimate the ratio of the QD sizes $l_L/l_S \sim 3$ because the period of the oscillations of the conductance is inversely proportional to the wire to back gate capacitance, here $c_{W-BG,L}$ and $c_{W-BG,S}$ are wire to back gate capacitances for large and small dots, respectively. The capacitance itself is proportional to the length of the wire forming the quantum dot $c_{W-BG,L}/c_{W-BG,S} \propto l_L/l_S$.

Fig.1b shows a scanning gate imaging of the device A. The value of the voltage applied to the back gate is $V_{BG} = 0$ V and to the tip $V_t = 1$ V. Equipotential lines mapped in the Fig.1b are slightly deformed because of the screening by metallic marker of the search pattern. The center dark region reveals the position of the center of the small quantum dot placed 0.35 μm apart from the right contact plate. This allows us to estimate the ratio of dots sizes from SGI as $l_L/l_S \sim 2$.

In Fig.3a the conductance as the function of V_{SD} and V_{BG} at low back gate voltages $-0.2 < V_{BG} < 2.3$ V of device B is presented. It is clearly visible that at $V_{BG} < 1.1$ V double Coulomb blockade diamond pattern is present while at higher back gate voltages only the single one survives. A calculation similar to the one performed for device A results for device B in a quantum dot sizes ratio of $l_L/l_S \sim 4$. At even higher back gate voltages $V_{BG} > 5.5$ V (cf. Fig.3b) no Coulomb blockade oscillations are present because all dots are open and the nonlinearity in conductance comes from a weak junction splitting nanowire B into two quantum dots.

In Fig.4a series of scanning gate images of device B is presented. The back-gate voltage is maintained a same value for all images ($V_{BG} = -1$ V) keeping the small QD near pinch off regime while the tip voltage is varied from scan to scan. V_t is of 3 V, 4 V and 5 V for scans (a), (b) and (c), respectively.

With increasing the tip voltage the number of the electrons in QD increases and the equipotential line of the first well pronounced Coulomb blockade conductance peak appears, see Fig.4b. The equipotential line from the second peak is clearly visible in Fig.4c. The conductance along the equipotential lines of the device B strongly depends on the position of the charged tip, see Fig.4b and 4c. The broken mirror-image symmetry of the conductance values along equipotential lines (mirror is placed on the axis of the wire) is the main experimental result of our paper and it will be discussed later in details.

The coincident centers of the equipotential curves reveals the position of the center of the small QD in the nanowire. The ratio of the dot sizes we estimated from the SGI experiment is $l_L/l_S \sim 3$.

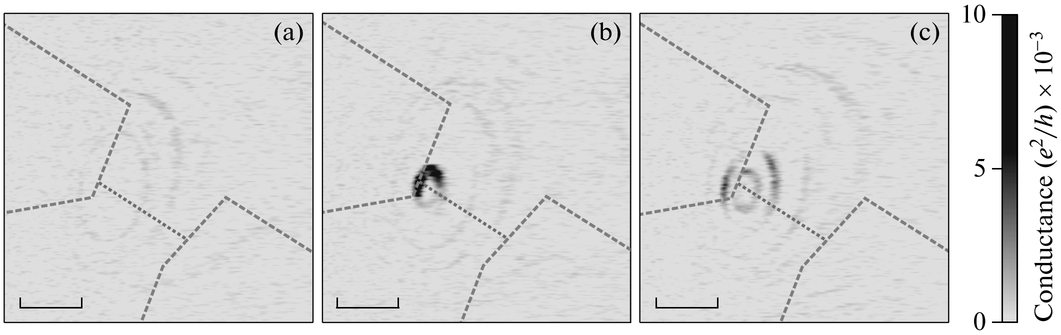

Fig.4. On images (a) to (c) the series of SGI of device B measured at 4.2 K is presented. The driving voltage of 0.1 mV is applied and the current is measured while the tip is scanning. The tip voltage is varied from scan to scan: V_t is of 3 V, 4 V and 5 V for scans (a), (b) and (c) correspondently. The back gate voltage is the same for all scans $V_{BG} = -1$ V. The scale bar corresponds to 1 μm for all three images. Dotted line denotes the wire position and dashed lines denote outline of metallic contacts

In both devices no special preparation of additional tunneling barriers was made to form the quantum dots. We attribute the presence of the barrier between the InAs wire and the metallic contact to the presence of residual contamination atoms at the interface. This barrier is presented according to the SGI measurements in the other samples from the same batch at the room temperature when the electronic system of the wire is almost depleted [20]. At a high electron density in the wire, which are induced by large back-gate voltages, the barriers disappear so that the dots become completely open at room temperature [20] as well as at $T = 4.2$ K (cf. Fig.3b). As mentioned previously, it was possible to extract the ratio of the dot sizes from the conduction map as well as from the SGI. The resulting values for device A are of 3 and 2, and for device B are of 4 and 3, respectively. We can explain some disagreement of the results with the presence of a depletion region nearby the contact areas because the presence of potential barriers affects smaller size quantum dots stronger.

The double Coulomb blockade pattern in Fig.2 disappears at low back gate voltages because the variation of the value of the total resistance ($R_{\text{tot}} = R_{SD}+R_{LD} = R_{SD}(1+R_{LD}/R_{SD})$) caused by oscillations of the large dot resistance value (R_{LD}) is masked by increasing of resistance of the small dot R_{SD} at low V_{BG} ($R_{LD} \ll R_{SD}$). Whereas, in Fig.3a the double Coulomb blockade pattern is found at low back gate voltages ($V_{BG} < 1.1$ V) only because at $V_{BG} > 1.1$ V larger quantum dot becomes open. Thus, a double Coulomb blockade pattern in devices A and B is only observable at quite narrow region of back gate voltages.

The alteration of the conductance of device B on the position of the charged tip scanned along the equipotential line (see Fig.4) can be governed both by the variation of large dot conductance (Coulomb blockade of the large dot [15, 12]) and by the variation of the tunneling rates through potential barriers of the small dot itself. We exclude the first scenario because the variation of the conductance observed in our experiment is too smooth. Equipotential lines governed by Coulomb blockade oscillations must be 4 times spatially denser from the large dot than from the small one [15, 12]. So the conductance deviation comes from altering of the tunneling rate of the QD blocking barriers. Moving the charged tip it is possible to change height of the barriers [13], but taking into account this mechanism only conductivity along the equipotential line might have mirror-image symmetry with the mirror placed on the wire axis. We do not observe this kind of symmetry of conductance in our experiment (see Fig.4). We attribute the observed broken symmetry shown in scanning gate images of device B to redistribution of the electrons density among conductive channels inside quantum wire. Different channels may have different tunneling rate through the blocking barriers so the redistribution of the electrons among them might result to alter the total conductance of the wire. This result is not very surprising because the mean free path in InAs wires is of 200 nm at room temperature [6].

In conclusion, we performed complex measurements at helium temperatures of two field-effect-transistors based on IsAs nanowires wires, each of the wire split into two QD with weak junction. To explain the deviation of the conductance of device B while the charged tip moved along the equipotential lines the redistribution of the electrons among conductive channels must be taken into account. Ratios of QD sizes extracted from conduction maps as function of V_{SD} and V_{BG} and from SGI measurements for both devices are in good agreement.

This work is supported by Russian Foundation for Basic Research, programs of the Russian Academy of Science, the Program for Support of Leading scientific Schools, and by International Bureau of the German Federal Ministry of Education and Research within the project RUS 09/052.

---

1. A. C. Ford, J. C. Ho, Yu-Lun Chueh et al., Nano Lett., **9** 360 (2009).
2. C. Thelander, T. Martensson, M. T. Bjork et al., Appl. Phys. Lett. **83**, 2052 (2003).
3. Th. Richter, Ch. Blomers, H. Luth et al., Nano Lett. **8**, 2834 (2008).
4. M. Scheffler, S. Nadj-Perge, Leo P. Kouwenhoven et al., J. Appl. Phys. **106**, 124303 (2009).
5. C. A. Mead and W. G. Spitzer, Phys. Rev. Lett. **10**, 471 (1963).
6. X. Zhou, S. A. Dayeh, D. Aplin et al., Appl. Phys. Lett. **89**, 053113 (2006).
7. R. Crook, C. G. Smith, A. C. Graham et al., Phys. Rev. Lett. **91**, 246803 (2003).
8. A. Pioda, S. Kicin, T. Ihn et al., Phys. Rev. Lett. **93**, 216801 (2004).
9. P. Fallahi, A. C. Bleszynski, R. M. Westervelt et al., Nano Lett. **5**, 223 (2005).
10. R. Crook, A. C. Graham, Ch. G. Smith et al., Nature **424**, 751 (1991).
11. M. A. Topinka, B. J. LeRoy, S. E. J. Shaw et al., Science **289**, 2323 (2000).
12. M. T. Woodside and P. L. McEuen, Science **296**, 1098 (2002).
13. A. A. Zhukov and G. Finkelstein, JETP Letters **89**, 212 (2009).
14. S. Schnez, J. Güttinger, M. Huefner et al., Phys. Rev. B **82**, 165445 (2010).
15. A. C. Bleszynski, F. A. Zwanenburg, R. M. Westervelt et al., Nano Lett. **7**, 2559 (2005).
16. E. P. A. M. Bakkers, J. A. VanDam, S. DeFrancheschi et al., Nat. Mater. **3**, 769 (2004).
17. A. A. Zhukov, Instrum. Exp. Tech. **51**, 130 (2008).
18. I. M. Ruzin, V. Chandrasechar, E. I. Levin *et al.*, Phys. Rev. B **45**, 13469 (1992).
19. F. R. Waugh, M. J. Berry, D. J. Mar et al., Phys. Rev. Lett. **75**, 705 (1995).
20. A. A. Zhukov, Ch. Volk, and Th. Schäpers, *Application of the rearrangeable local Coulomb potential profile for investigation of conductivity of InAs wires*, preprint.